DMD Fast Forward. Published on December 23, 2015 as DOI: 10.1124/dmd.115.068429
This article has not been copyedited and formatted. The final version may differ from this version.

Functional comparison of human colonic carcinoma cell lines and primary small intestinal epithelial cells for investigations of intestinal drug permeability and first-pass metabolism

Yoshiyuki Yamaura, Brian D. Chapron, Zhican Wang, Jonathan Himmelfarb and Kenneth E. Thummel

Department of Pharmaceutics (Y.Y., B.D.C., Z.W. and K.E.T.) and Nephrology (J.H.), University of Washington, Seattle, Washington, USA

Running title: *In vitro* characterization of human intestinal cell models

Corresponding author

Kenneth E. Thummel

Department of Pharmaceutics, University of Washington, Seattle WA 98195-7610

Phone: +1-206-543-0819

Fax: +1-206-543-3204

Email: thummel@u.washington.edu

Number of text pages: 25

Number of tables: 0

Number of figures: 5

Number of supplemental tables: 1

Number of supplemental figures: 2

Number of references: 25

Number of words in the Abstract: 243

Number of words in the Introduction: 612

Number of words in the Discussion: 942

Abbreviations: 5-aza-dC, 5-aza-2'-deoxycytidine; BCRP, breast cancer resistance protein; CYP3A4, Cytochrome P450 3A4; DDI, drug-drug interactions; DMEM, high glucose Dulbecco's modified eagle medium with L-glutamine; DMEM/F12, 50:50 Dulbecco's modified eagle medium with Ham's F-12; DMSO, Dimethyl sulfoxide; d4-1'-OH MDZ, d_4-1'-hydroxymidazolam; d_4-MDZ, d_4-midazolam; DPBS, Dulbecco's phosphate-buffered saline, with no calcium or magnesium; $DPBS^{++}$, Dulbecco's phosphate-buffered saline with calcium and magnesium; FBS, fetal bovine serum; fSIEC, fetal human small intestinal epithelial cells; GAPDH, glyceraldehyde 3-phosphate dehydrogenase; HBSS, Hank's balanced salt solution; IgG, Immunoglobulin G; ISTD, internal standard; LC–MS/MS, liquid chromatography coupled with tandem mass spectrometry; MDR1, multidrug resistance 1; MDZ, midazolam; MEM, minimum essential medium; MRM, multiple reaction monitoring; MRP2, multidrug resistance-associated protein 2; NEAA, MEM non-essential amino acids; $1\alpha,25(OH)_2D_3$, 1α,25-dihydroxyvitamin D_3; 1´-OH MDZ, 1´-hydroxymidazolam; OCT1, organic cation transporter 1; P_{app}, apparent permeability coefficient; PCR, polymerase chain reaction; PTB, PBS containing 0.1% Triton X-100 and 5% BSA; PXR, pregnane X receptor; qRT-PCR, quantitative real-time PCR; TEER, trans-epithelial electrical resistance; UGT1A1, UDP glucuronosyltransferase 1A1; VDR, vitamin D receptor; ZO-1, zonula occludens-1;

Abstract

To further the development of a model for simultaneously assessing intestinal absorption and first-pass metabolism *in vitro*, Caco-2, LS180, T84 and fSIEC were cultured on permeable inserts and the integrity of cell monolayers, CYP3A4 activity and the inducibility of enzymes and transporters involved intestinal drug disposition were measured. Caco-2, T84 and fSIEC all formed tight junctions, as assessed by immunofluorescence microscopy for zonula occludens-1 (ZO-1), which was well organized into circumscribing strands in T84, Caco-2 and fSIEC, but was diffuse in LS180 cells. The TEER value for LS180 monolayers was lower than that for Caco-2, T84 and fSIEC. In addition, the apical-to-basolateral permeability of the paracellular marker, lucifer yellow, across LS180 monolayers was higher than in fSIEC, T84 and Caco-2 monolayers. The transcellular marker, propranolol exhibited similar permeability across all cells. With regard to metabolic capacity, T84 and LS180 cells showed comparable basal midazolam hydroxylation activity and it was inducible by rifampin and $1\alpha,25(OH)_2D_3$ in LS180 cells, but only marginally so in T84 cells. The basal CYP3A4 activity of fSIEC and Caco-2 cells was much lower and not inducible. Interestingly, some of the drug transporters expressed in LS180 and Caco-2 cells were induced by either $1\alpha,25(OH)_2D_3$ or rifampin or both, but there were only limited effects in the other two cell lines. These results suggest that none of the cell lines tested fully replicated the drug disposition properties of the small intestine and that the search for an ideal screening tool must continue.

Introduction

Within the pharmaceutical industry, the oral bioavailability of lead compounds is frequently optimized by enhancing intestinal permeability and reducing first-pass metabolism. Caco-2 cell monolayers are routinely used as an *in vitro* intestinal permeability screening model. The permeability of drugs across Caco-2 monolayers have been shown to correlate well with the percent of drug absorbed in humans for both passively absorbed and actively transported compounds (Artursson and Karlsson, 1991; Yee, 1997). However, Caco-2 cells do not robustly express CYP3A4 under standard culturing conditions (Schmiedlin-Ren et al., 1997). CYP3A4 metabolizes a wide range of chemically diverse compounds. Moreover, the enzyme is the most abundant drug-metabolizing P450 in the small intestine (Paine et al., 2006) and participates in first-pass metabolism of drugs (Kato, 2008). Consequently, CYP3A4 is an important enzyme when considering the potential for DDI at the site of the intestinal epithelium (Peters et al., 2012).

The deficiency of CYP3A4 expression in Caco-2 cells makes them a poorly suited model for studying intestinal first-pass metabolism and DDI. To resolve this deficiency, some groups have tried to transfect Caco-2 cells with CYP3A4 cDNA (Brimer et al., 2000; Crespi et al., 2000). However, the resultant expression of CYP3A4 protein was relatively low and unstable in these transfected cells. It has also been reported that CYP3A4 expression levels can be induced by treatment of a Caco-2 cell subclone with $1\alpha,25(OH)_2D_3$ (Schmiedlin-Ren et al., 1997). This model has been used to examine first-pass metabolism of midazolam (Fisher et al., 1999) and saquinavir (Mouly et al., 2004). However, CYP3A4 expression in these cells is still relatively low compared to human duodenal mucosa (Paine et al., 1996; Fisher et al., 1999). Furthermore, these Caco-2 subclones require culturing for an additional two weeks post confluence in order for induction and differentiation to occur. As such, experiments using these cells can be time-consuming and not compatible with high-

throughput screening of numerous compounds. Additionally, the baseline-induced Caco-2 subclone does not undergo further induction of CYP3A4 by rifampin or other prototypical inducers (Schmiedlin-Ren et al., 2001).

Other colonic carcinoma cells lines such as LS180 and T84 cells could potentially provide a viable alternative for simultaneously assessing the intestinal permeability and first-metabolism of drugs. Although LS180 cells exhibit basal and inducible CYP3A4 activity (Zheng et al., 2012), they are thought not to form tight junctions in culture. In contrast, T84 cells are known to form tight junctions (Dharmsathaphorn et al., 1984). However, expression of CYP3A4 by T84 cells is controversial (Juuti-Uusitalo et al., 2006; Bourgine et al., 2012) and its inducibility has not been reported. It is worth noting that this cell line expresses PXR, which is one of the important nuclear transcription factors mediating CYP3A4 induction. Additionally, induction of the efflux transporter P-glycoprotein (MDR1) been observed in T84 cells treated with the PXR ligand, rifampin (Haslam et al., 2008).

The growing commercial availability of primary fetal human small intestinal epithelial cells (fSIEC) provides a unique alternative to immortal colon cancer cell lines. While some work has been done to characterize the pharmacokinetic properties of both stem-cell derived and primary human intestinal epithelial cells (Kauffman et al., 2013), little is known about the metabolic properties with respect to CYP3A4 activity. Additionally, it is not known whether the primary human intestinal cells evaluated in the literature are specifically sourced from the small intestine or if they originate from the colon.

In the present study, we evaluated LS180, T84, Caco-2 and fSIEC to further the development of an *in vitro* model for the simultaneous assessment of intestinal permeability and first-pass metabolism. To characterize these cells, we examined TEER, tight junction protein localization, CYP3A4-mediated metabolism and induction of mRNA transcripts coding for proteins related to intestinal drug disposition.

DMD Fast Forward. Published on December 23, 2015 as DOI: 10.1124/dmd.115.068429
This article has not been copyedited and formatted. The final version may differ from this version.

Materials and Methods

Chemicals and reagents. Rifampicin, 5-aza-dC, bovine serum albumin, cell dissociation solution for LS180 cells, PCR primer pairs (BCRP, MDR1, MRP2 and OCT1), HBSS, HEPES buffer, Triton X-100, propranolol, atenolol and furosemide were purchased from Sigma-Aldrich (St. Louis, MO). D-Sucrose was obtained from Fisher Scientific (Itasca, IL). 16% Formaldehyde (methanol free) was purchased from polysciences (Warrington, PA). $1\alpha,25(OH)_2D_3$ was obtained from Calbiochem (La Jolla, CA). MDZ, d_4-MDZ and d4-1´-OH MDZ were purchased from Cerilliant (Round Rock, TX). 1´-OH MDZ was purchased from Ultrafine (Manchester, UK). DPBS, $DPBS^{++}$, MEM, DMEM/F12, DMEM, penicillin-streptomycin, NEAA, TRIzol reagent, High Capacity cDNA Reverse Transcription Kit with RNase Inhibitor, Power SYBR green PCR master mix, PCR primer pairs (CYP3A4, GAPDH, PXR, UGT1A1 and VDR), Rabbit polyclonal anti-ZO-1 antibody (cat#402200), Alexa Fluor 488 Donkey anti-rabbit IgG, ProLong Gold Antifade reagent with DAPI and lucifer yellow biocytin were obtained from Life technologies (Carlsbad, CA). FBS was purchased from Atlanta Biologicals (Lawrenceville, GA). Sodium pyruvate and Trypsin EDTA were purchased from Cellgro (Herindon, VA). Cell dissociation solution for fSIEC, epithelial pro-conditioned media and vessel coating solution were purchased from DV Biologics (Costa Mesa, CA).

Cell culture. LS180 (passage 25-34), T84 (passage 56-66) and Caco-2 cells (passage 26-35) were obtained from American Type Culture Collection (Manassas, VA). fSIEC, 14.9 weeks gestational age, were obtained from DV Biologics (Costa Mesa, CA) and experiments were conducted at passage 3-8. Cells were maintained at 37°C in a humidified incubator with 5% CO_2. LS180 cells were cultured in MEM supplemented with 10% FBS, 1% penicillin-

DMD Fast Forward. Published on December 23, 2015 as DOI: 10.1124/dmd.115.068429
This article has not been copyedited and formatted. The final version may differ from this version.

streptomycin and 1% sodium pyruvate. T84 cells were cultured in DMEM/F12 supplemented with 10% FBS and 1% penicillin-streptomycin. Caco-2 cells were cultured in DMEM supplemented with 10% FBS, 1% penicillin-streptomycin and 1% NEAA. fSIEC were cultured in epithelial pro-conditioned media (DV Biologics, Costa Mesa, CA, cat#D-Pro-015-100). The cells were passaged by addition of cell dissociation solutions (for LS180 and fSIEC) or trypsin EDTA (for T84 and Caco-2) at 80% confluence. Cells were seeded onto polyethylene-terephthalate, 0.4 μm pore size filter inserts for 24 well plates (0.3 cm^2 growth area (BD Biosciences, Franklin Lakes, NJ, cat#353095), or 0.336 cm^2 growth area (Greiner bio-one, Monroe, NC, cat#662641) at a density of 5×10^5 cells/cm^2 and maintained by changing medium two or three times a week. For the experimental treatment, the medium was removed and the cells were washed twice with $DPBS^{++}$ and then treated with medium containing the compound or vehicle for 48 hours. Stock solutions of rifampicin (50 mM) and 1α,25$(OH)_2D_3$ (1 μM) were prepared in DMSO and ethanol, respectively and were diluted 1000-fold in medium. All FBS used during experimental treatment was resin-charcoal-treated. To examine epigenetic mechanisms, T84 cells were treated with vehicle (0.1% DMSO) or 5-aza-dC at concentrations of 0.2 to 20 μM for 24 hours before treatment with rifampicin and 1α,25$(OH)_2D_3$.

CYP3A4 activity assessment. After an experimental treatment, cells were washed twice with $DPBS^{++}$, then 0.3 mL of culture medium containing midazolam (MDZ) at a final concentration of 8 μM (0.1% DMSO) was added to the filter insert (apical compartment) and 0.7 mL of medium without MDZ was added to the basolateral compartment. The cells were incubated for 60 min, then apical and basolateral media were collected and stored at -80 °C. MDZ and 1´-OH MDZ were measured using LC-MS/MS on an Agilent 6410 QQQ equipped with HPLC1290 system (Agilent Technologies, Palo Alto, CA). After thawing, 10 μL of each

DMD Fast Forward. Published on December 23, 2015 as DOI: 10.1124/dmd.115.068429
This article has not been copyedited and formatted. The final version may differ from this version.

sample (apical samples were 5-fold diluted with blank media) were mixed with 20 μL of methanol and 100 μL of internal standard (ISTD) solution containing 5 ng/mL d4-MDZ and 10 ng/mL d4-1´-OH MDZ in acetonitrile. A series of dilutions of MDZ and 1'-OH MDZ standards were prepared in methanol as stock solutions and stored at -80 °C. The standard curve samples were prepared by mixing 10 μL of each these stock solutions and 10 μL of blank medium, and then adding 100 μL of ISTD solution. The samples were then centrifuged for 5 min at 12,000 x *g* and 10 μL of the supernatant was analyzed via LC/MS-MS. Chromatographic separations were achieved with a Zorbax SB-C18, 5 μm, 2.1×150 mm column (Agilent Technologies) using 10 mM ammonium acetate (pH 4.0) (A) and acetonitrile (B) as a mobile phase. The flow rate was 0.25 mL/min with a gradient as follows: 45% B for 1.5 min, then increased to 80% linearly over 2.5 min, held at 80% for 2 min, then equilibrated back to 45% for 2 min. The following MRM transitions were monitored: m/z 326.0 > 291.2 for MDZ, m/z 330.0 > 295.0 for d4-MDZ, m/z 342.0 > 168.1 for 1'-OH MDZ and m/z 346.0 > 168.0 for d4-1'-OH MDZ in the positive ion mode.

RNA isolation and qRT-PCR analysis. After experimental treatment, cells collected from each insert were homogenized in 0.25 mL of TRIzol reagent and stored at -80 °C. Total cellular RNA was isolated according to the manufacturer-supplied protocol for TRIzol reagent. The isolated RNA was dissolved in nuclease-free water and the concentration was determined using a Nanodrop spectrophotometer ND-1000 (Thermo Scientific, Wilmington, DE). Reverse transcription was performed according to the manufacturer's instructions for the high capacity cDNA reverse transcription kit. For each reaction, 2 μg of isolated RNA was mixed with dNTP, random hexamer primers, RNase inhibitor and MultiScribe reverse transcriptase in reaction buffer in a total volume of 20 μL. The reverse transcription condition was set as 25 °C for 10 min, 37 °C for 120 min and 85 °C for 5 s, using a PTC-200 DNA

DMD Fast Forward. Published on December 23, 2015 as DOI: 10.1124/dmd.115.068429
This article has not been copyedited and formatted. The final version may differ from this version.

engine cycler (Bio-Rad, Hercules, CA). qRT-PCR was performed using gene-specific primers and the Power SYBR green master mix with a ABI 7900HT system (Applied Biosystems, Bedford, MA). The PCR mixture consisted of 1 μL of cDNA, gene-specific forward and reverse primers (20 pmol each), Power SYBR green master mix and nuclease-free water, in a total volume of 20 μL for each reaction. The following program was used: a denaturation step at 95 °C for 10 min, 40 cycles of PCR (denaturation 95 °C for 30 s; annealing 65 °C for 30 sec; and extension 72 °C for 30 s), followed by 72 °C for 5 min and then a dissociation/melting step (95 °C for 15 s, 65 °C for 15 s, 95 °C for 15 s, 25 °C for 5 min). All tested gene products were quantified using the comparative ΔΔCt calculation for relative quantification of gene expression, normalized to GAPDH. A list of the primer sets is provided in Supplemental Table 1.

Immunocytochemistry and confocal microscopy. Cell monolayers grown on filter inserts were washed twice with $DPBS^{++}$, fixed in 4% formaldehyde in $DPBS^{++}$ containing 2% sucrose for 15 min at room temperature, washed twice with $DPBS^{++}$ and then incubated in 50 mM NH_4Cl for 30 min to quench unreacted aldehyde groups. The cells were washed twice more with $DPBS^{++}$ and then blocked and permeabilized in PTB for 30 min. Subsequently, the cells were incubated with a 500-fold dilution of primary antibody (rabbit anti-ZO-1) in PTB for 30 min at room temperature or overnight at 4 °C. The cell monolayers were then washed three times with $DPBS^{++}$ and incubated with a 1000-fold dilution of fluorescent-conjugated secondary antibody (Alexa Fluor 488 Donkey anti-rabbit IgG) in PTB for 30 min at room temperature. After washing with $DPBS^{++}$ three additional times, the filters were cut out from their plastic inserts and placed on glass microscope slides. The inserts were then mounted with ProLong Gold Antifade reagent with DAPI and analyzed on a Nikon A1 confocal microscope (Nikon, Melville, NY).

DMD Fast Forward. Published on December 23, 2015 as DOI: 10.1124/dmd.115.068429
This article has not been copyedited and formatted. The final version may differ from this version.

TEER measurement. Cell monolayer integration was evaluated by measuring the TEER using a Millicell ERS (Millipore, Bedford, MA). For a given set of cultures, a single filter insert without cells was measured for background resistance. TEER was determined as the product of the background-corrected resistance and the growth area of the insert.

Permeability assay. The cell monolayers were washed with transport buffer (10mM HEPES in HBSS, pH 7.4) and maintained at 37 °C until use. Stock solutions of test compound (lucifer yellow (60 mM), propranolol (20 mM) and atenolol (60 mM)) were prepared in DMSO and diluted 200-fold in transport buffer to make compound solution (final concentrations were 300 μM, 100 μM and 300 μM, respectively). For the lucifer yellow permeability measurement, 0.3 mL of compound solution was added to filter insert, while 0.7 mL of receiver buffer (transport buffer containing 0.5% DMSO) was added to the basolateral compartment. After 60 min incubation at 37°C, 300 μL of aliquots were withdrawn from basolateral compartment. The samples were analyzed by fluorescence detection using a Spectra MAX-Gemini XS microplate reader (Molecular Devices, Sunnyvale, CA) with excitation filter at 485 nm and emission filter at 538 nm. For propranolol and atenolol permeability measurement, 0.32 mL of compound solutions were added to filter inserts, while 0.7 mL of receiver buffer were added to the basolateral compartment. 20 μL of aliquots were withdrawn from the insert at 0 min, 70 μL of aliquots were withdrawn from the basolateral compartment and replaced with an equal volume of receiver buffer: at 15 to 60 min for propranolol; at 60 to 120 min for atenolol. Then 20 μL of aliquots were withdrawn from the insert. The samples were stored at -80°C until analysis. Propranolol and atenolol were measured using LC-MS/MS on an Agilent 6410 QQQ equipped with UPLC1290 system. After thawing, 50 μL of samples (apical samples were 100-fold, basolateral samples of

propranolol were 5-fold diluted with blank receiver buffer) were mixed with 50 μL of ISTD solution (furosemide, 25 μg/mL in acetonitrile). A series of dilutions of propranolol and atenolol standards were prepared in methanol as stock solutions and stored at -80 °C. The standard curve samples were prepared by mixing 5 μL of stock solution and 50 μL of blank receiver buffer, and then mixed with 50 μL of ISTD solution. 20 μL of the samples was analyzed. Chromatographic separations were achieved with a Zorbax SB-C18, 5 μm, 2.1×150 mm column (Agilent Technologies) using 10 mM ammonium acetate (pH 4.0) (A) and acetonitrile (B) as a mobile phase. The flow rate was 0.25 mL/min with a gradient as follows: 25% B for 1.5 min, then increased to 75% linearly over 2 min, held at 75% for 4.5 min, then equilibrated back to 25% for 4 min. The following MRM transitions were monitored: *m/z* 260.31 > 116.1 for propranolol, *m/*z 267.31 > 145 for atenolol in the positive ion mode, *m/z* 329.7 > 285.9 for furosemide in the negative ion mode.

Determination of permeability coefficient of permeability marker compounds. The P_{app} (cm/s) for each marker compound was calculated according to following equation:

$$P_{app} = \frac{dQ}{dt} \cdot \frac{1}{AC_0}$$

where dQ/dt is the rate of compound transfer (pmol/s) into the basolateral compartment under sink conditions (where less than 20% of the compound was transferred across the cell monolayer), A is the surface area of the filter insert (cm^2), and C_0 is the initial concentration of the compound in the apical compartment.

Statistical analysis. Data are presented as mean ± S.D. The effect of rifampicin and 1α,25$(OH)_2D_3$ on midazolam 1´-hydroxylation and mRNA expression levels was assessed by comparison to vehicle controls and presented as the mean ± S.D.. Overall standard deviation for ratios of two means with independent standard deviations was calculated using a propagation of error equation. Statistical significance ($\alpha = 0.05$) was determined via unpaired t-tests. All statistical analyses were conducted using GraphPad Prism version 5.04 (GraphPad Software, La Jolla, CA).

DMD Fast Forward. Published on December 23, 2015 as DOI: 10.1124/dmd.115.068429
This article has not been copyedited and formatted. The final version may differ from this version.

Results

Induction of CYP3A4 metabolic activity in cultured epithelial cells. The effects of the prototypical PXR ligand, rifampicin, and the VDR ligand, 1α,25$(OH)_2D_3$, on MDZ 1´-hydroxylation in cells cultured on permeable inserts are shown in Fig. 1. LS180 cells showed basal CYP3A4 activity that was significantly induced by both rifampicin and 1α,25$(OH)_2D_3$ as previously reported (Fisher et al., 1999). T84 cells showed basal CYP3A4 activity that was comparable to LS180 cells. However, their inducibility through both PXR and VDR pathways was much lower than that seen with LS180 cells. It was confirmed that Caco-2 cells do not possess substantial levels of basal CYP3A4 activity (Artursson and Karlsson, 1991). Furthermore, both rifampicin and 1α,25$(OH)_2D_3$ failed to significantly increase 1´-OH-MDZ formation in Caco-2 cells. fSIEC demonstrated similarly low and poorly inducible CYP3A4 activity to that of Caco-2 cells.

Induction of mRNA expression. The effects of rifampicin and 1α,25$(OH)_2D_3$ on gene expression are shown in Fig. 2. In summary, statistically significant increases in CYP3A4 mRNA was observed with both rifampicin and 1α,25$(OH)_2D_3$ treatment of LS180 cells. There was also a significant induction of MRP2 mRNA observed in LS180 cells treated with 1α,25$(OH)_2D_3$ but not rifampicin. In T84 cells, the only statistically significant change was a 2.2 fold-increase in BCRP mRNA after treatment with rifampicin. We did not observe an induction of MDR1 mRNA transcripts with rifampin treatment, as has been observed previously (Haslam et al., 2008). Overall, T84 cells response to the inducing agents appeared to be more muted and less variable than the other candidate cells. Caco-2 cells showed statistically significant 4.5-fold increase in OCT1 mRNA after 1α,25$(OH)_2D_3$ treatment. Caco-2 cells also experienced a statistically significant 17% decrease in UGT1A1 mRNA following treatment with 1α,25$(OH)_2D_3$. In general, the induction of mRNA transcripts in

DMD Fast Forward. Published on December 23, 2015 as DOI: 10.1124/dmd.115.068429
This article has not been copyedited and formatted. The final version may differ from this version.

Caco-2 cells appeared to be more sensitive to $1\alpha,25(OH)_2D_3$ than rifampicin treatment. Finally, a statistically significant 50-fold decrease in BCRP mRNA was observed in fSIEC treated with $1\alpha,25(OH)_2D_3$.

Cell monolayer integrities. The time-dependence of TEER values for three cell lines are shown in Fig. 3. The TEER values for Caco-2 and T84 cells reached approximately 500 and 2000 $\Omega \cdot cm^2$, respectively, after about 10 days. In contrast, LS180 cells showed much lower TEER values, at about 15 $\Omega \cdot cm^2$ throughout the 18-day experimental period. At 50 $\Omega \cdot cm^2$, TEER values for fSIEC were slightly higher than LS180 cells. However, integrity of tight junctions appeared to weaken over time in the fSIEC monolayers, dropping closer to that of LS180 cells after 14 days in culture.

Drug permeability. Permeability of the paracellular marker compound, lucifer yellow, was comparably low (less than 1×10^{-6} cm/s) in all cell types except LS180 (Fig 4). Propranolol permeability was similar across all 4-cell types. Atenolol permeability was low in T84 and Caco-2 cells but much higher in LS180 and, especially, fSIEC.

Immunocytochemistry. Distribution of tight junction protein ZO-1 was well organized into circumscribing strands in fSIEC, T84 and Caco-2 cells, but was more diffuse in LS180 cells (Fig 5). An intracellular region showed some stronger signal in the LS180 cells. This could perhaps suggest a Golgi apparatus localization of the protein, but no efforts to confirm this possibility were undertaken.

Discussion

The development of a high-throughput *in vitro* system to simultaneously assess intestinal drug-transport and metabolism is crucial to improving our understanding the role of the intestine in drug disposition. Through the experiments outlined in this paper, we have explored three candidate cell sources (LS180, T84 and fSIEC) as alternatives to the traditional Caco-2 monolayers that have been plagued by poor and variable CYP3A4 enzymatic activity (Schmiedlin-Ren et al., 1997; Brimer et al., 2000; Crespi et al., 2000). Our results confirmed the limitations of the monolayers of Caco-2 and LS180 cells. We demonstrated that LS180 cells robustly express CYP3A4 and that such expression is inducible by both rifampicin and $1\alpha,25(OH)_2D_3$. However, their lack of tight junction formation permits an unacceptably high degree of paracellular transport, as evidenced by the permeability of lucifer yellow across LS180 cell monolayers cultured on permeable inserts. The high degree of permeability also seen with the hydrophilic compound, atenolol, is likely due to extensive paracellular flux. While LS180 monolayers may be suitable for drug-metabolism and induction studies, they would not make suitable candidates for the simultaneous assessment of permeability and drug transport and potential functional interplay between those processes. Alternatively, T84 cells seem to express both basal CYP3A4 activity and tight junctions. As such, monolayers of these cells could theoretically be used to simultaneously explore passive transcellular drug permeability and CYP3A4-mediated metabolism. However, $1\alpha,25(OH)_2D_3$-mediated induction of CYP3A4 activity and mRNA expression in T84 cells was much lower than that of LS180 cells despite a modest, but significant 1.7-fold greater expression of VDR mRNA in T84 cells as compared to LS180 cells (Supplemental Figure 1). In a second post-hoc analysis, PXR mRNA expression was

also shown to differ between the two cells lines, with an approximately 2-fold higher expression in LS180 cells over T84 cells.

To explore the mechanisms underlying a lack of inducibility of T84 cells, we examined epigenetic mechanisms by the treatment of the cells with varying concentrations of the DNA methylation inhibitor, 5-aza-dC. No marked effect on CYP3A4 mRNA expression was observed (Supplemental Figure 2) thus further studies are needed to understand this cellular characteristic. A lack of inducibility of CYP3A4 in these cells is a technical limitation, however, they hold potential as an improvement upon Caco-2 monolayers, particularly for compounds where reduced bioavailability from basal CYP3A4-mediated first-pass metabolism is a concern.

As a novel approach, we also explored using fSIEC to recapitulate the intestinal epithelial barrier. We confirmed low CYP3A4 expression in fSIEC as previously reported in fetal proximal small bowel sections (Johnson et al., 2001) and additionally demonstrated that the CYP3A4 was much less inducible by rifampicin and $1\alpha,25(OH)_2D_3$. Low permeability of lucifer yellow, combined with the observation of circumscribing strands of ZO-1 signal upon immunocytochemistry staining, confirmed the presence of tight junctions in fSIEC monolayers. At approximately 50 $\Omega \cdot cm^2$, TEER values for the fSIEC monolayers were substantially less than that of T84 or Caco-2 but strikingly close to the 40 $\Omega \cdot cm^2$ reported for human small intestine in an Ussing chamber (Sjoberg et al., 2013). This is in contrast to the slightly higher 100 $\Omega \cdot cm^2$ seen in fSIEC monolayers derived from adult intestinal stems cells or the 200 $\Omega \cdot cm^2$ seen in those derived from induced pluripotent stem cells (iPSC) (Kauffman et al., 2013; Takenaka et al., 2014). In addition to iPSC-derived SIEC, Kauffman et al. also assessed TEER values in primary human intestinal epithelial cells from an unstated region of the intestine. Monolayers of these primary cells produced a TEER values exceeding 1500 $\Omega \cdot cm^2$, suggesting a colonic, rather than small intestinal origin (Powell, 1981). Despite

similar lucifer yellow permeability to T84 and Caco-2 cells, the mean apparent permeability for atenolol was much higher in fSIEC monolayers. This could point to a reduction in transporter-mediated efflux processes or an increase in active uptake of atenolol in fSIEC over T84, Caco-2 or LS180 cells. Despite its very poor permeability, atenolol has a moderate oral bioavailability at 50% (Kirch and Gorg, 1982). It is also reported that the systemic exposure to atenolol is markedly reduced by apple juice ingestion, a phenomena attributed to the inhibition of intestinal OATP2B1 by constituents present in apple juice (Jeon et al., 2013). It is possible that a system possessing more *in vivo*-like expression of uptake transporters could help serve as a useful tool in preventing the needless abandonment of compounds with poor passive permeability, but which would still have sufficient bioavailability *in vivo*. It is also worth noting that while atenolol transport across Caco-2 monolayers was poor, there was a 4.5-fold induction in OCT1 mRNA after treating Caco-2 cells with $1\alpha,25(OH)_2D_3$. Further exploration of inducibility of transporters involved in the uptake of organic cations such as atenolol in traditional Caco-2 cells may be warranted.

As a whole, the experiments outlined herein confirm the poor suitability of both LS180 and Caco-2 cells for the simultaneous assessment of intestinal permeability and first-pass CYP3A4-mediated metabolism. T84 cells may present as a useful cell model for this role but have a shortcoming in their insensitivity to the induction of CYP3A4 by both rifampin and $1\alpha,25(OH)_2D_3$**.** fSIEC monolayers formed tight junctions, possessing a comparable TEER to that seen in the human small intestine. This makes them an attractive candidate for studies of intestinal permeability. However, the low activity of CYP3A4 makes monolayers of these cells poorly suited for the complex assessment of first-pass intestinal metabolism and permeability. With the rising interest in developing 3-dimensional microphysiological cell culture systems, there is the hope that a more faithful recapitulation of the native *in vivo* environment will help retain the necessary phenotype for the *in vitro*

DMD Fast Forward. Published on December 23, 2015 as DOI: 10.1124/dmd.115.068429
This article has not been copyedited and formatted. The final version may differ from this version.

assessment of the enterocytes role in first-pass metabolism and absorption of xenobiotics *in vitro*.

Acknowledgments

We would like to thank Dr. Edward J Kelly and Ron Seifert for their assistance and expertise in confocal microscopy imaging.

Authorship Contributions

Participated in research design: Yamaura, Chapron, Wang, Himmelfarb and Thummel

Conducted experiments: Yamaura, Chapron and Wang

Performed data analysis: Yamaura and Chapron

Wrote or contributed to the writing of the manuscript: Yamaura, Chapron and Thummel

References

Artursson P and Karlsson J (1991) Correlation between oral drug absorption in humans and apparent drug permeability coefficients in human intestinal epithelial (Caco-2) cells. *Biochem Biophys Res Commun* **175:**880-885.

Bourgine J, Billaut-Laden I, Happillon M, Lo-Guidice JM, Maunoury V, Imbenotte M, and Broly F (2012) Gene expression profiling of systems involved in the metabolism and the disposition of xenobiotics: comparison between human intestinal biopsy samples and colon cell lines. *Drug Metab Dispos* **40:**694-705.

Brimer C, Dalton JT, Zhu Z, Schuetz J, Yasuda K, Vanin E, Relling MV, Lu Y, and Schuetz EG (2000) Creation of polarized cells coexpressing CYP3A4, NADPH cytochrome P450 reductase and MDR1/P-glycoprotein. *Pharm Res* **17:**803-810.

Crespi CL, Fox L, Stocker P, Hu M, and Steimel DT (2000) Analysis of drug transport and metabolism in cell monolayer systems that have been modified by cytochrome P4503A4 cDNA-expression. *Eur J Pharm Sci* **12:**63-68.

Dharmsathaphorn K, McRoberts JA, Mandel KG, Tisdale LD, and Masui H (1984) A human colonic tumor cell line that maintains vectorial electrolyte transport. *Am J Physiol* **246:**G204-208.

Fisher JM, Wrighton SA, Watkins PB, Schmiedlin-Ren P, Calamia JC, Shen DD, Kunze KL, and Thummel KE (1999) First-pass midazolam metabolism catalyzed by 1alpha,25-dihydroxy vitamin D3-modified Caco-2 cell monolayers. *J Pharmacol Exp Ther* **289:**1134-1142.

Haslam IS, Jones K, Coleman T, and Simmons NL (2008) Rifampin and digoxin induction of MDR1 expression and function in human intestinal (T84) epithelial cells. *Br J Pharmacol* **154:**246-255.

Jeon H, Jang IJ, Lee S, Ohashi K, Kotegawa T, Ieiri I, Cho JY, Yoon SH, Shin SG, Yu KS,

and Lim KS (2013) Apple juice greatly reduces systemic exposure to atenolol. *Br J Clin Pharmacol* **75:**172-179.

Johnson TN, Tanner MS, Taylor CJ, and Tucker GT (2001) Enterocytic CYP3A4 in a paediatric population: developmental changes and the effect of coeliac disease and cystic fibrosis. *Br J Clin Pharmacol* **51:**451-460.

Juuti-Uusitalo KM, Kaukinen K, Maki M, Tuimala J, and Kainulainen H (2006) Gene expression in TGFbeta-induced epithelial cell differentiation in a three-dimensional intestinal epithelial cell differentiation model. *BMC Genomics* **7:**279.

Kato M (2008) Intestinal first-pass metabolism of CYP3A4 substrates. *Drug Metab Pharmacokinet* **23:**87-94.

Kauffman AL, Gyurdieva AV, Mabus JR, Ferguson C, Yan Z, and Hornby PJ (2013) Alternative functional in vitro models of human intestinal epithelia. *Front Pharmacol* **4:**79.

Kirch W and Gorg KG (1982) Clinical pharmacokinetics of atenolol--a review. *Eur J Drug Metab Pharmacokinet* **7:**81-91.

Mouly SJ, Paine MF, and Watkins PB (2004) Contributions of CYP3A4, P-glycoprotein, and serum protein binding to the intestinal first-pass extraction of saquinavir. *J Pharmacol Exp Ther* **308:**941-948.

Paine MF, Hart HL, Ludington SS, Haining RL, Rettie AE, and Zeldin DC (2006) The human intestinal cytochrome P450 "pie". *Drug Metab Dispos* **34:**880-886.

Paine MF, Shen DD, Kunze KL, Perkins JD, Marsh CL, McVicar JP, Barr DM, Gillies BS, and Thummel KE (1996) First-pass metabolism of midazolam by the human intestine. *Clin Pharmacol Ther* **60:**14-24.

Peters SA, Schroeder PE, Giri N, and Dolgos H (2012) Evaluation of the use of static and dynamic models to predict drug-drug interaction and its associated variability: impact

on drug discovery and early development. *Drug Metab Dispos* **40:**1495-1507.

Powell DW (1981) Barrier function of epithelia. *Am J Physiol* **241:**G275-288.

Reckhow D (2004) Chapter XXIII: Parametric Statistics, in: *Enviromental Engineering Analysis*, UMASS College of Engineering. Available: http://www.ecs.umass.edu/cee/reckhow/courses/572/572bk23/572BK23.html [Accessed September 24, 2015.]

Schmiedlin-Ren P, Thummel KE, Fisher JM, Paine MF, Lown KS, and Watkins PB (1997) Expression of enzymatically active CYP3A4 by Caco-2 cells grown on extracellular matrix-coated permeable supports in the presence of 1alpha,25-dihydroxyvitamin D3. *Mol Pharmacol* **51:**741-754.

Schmiedlin-Ren P, Thummel KE, Fisher JM, Paine MF, and Watkins PB (2001) Induction of CYP3A4 by 1 alpha,25-dihydroxyvitamin D3 is human cell line-specific and is unlikely to involve pregnane X receptor. *Drug Metab Dispos* **29:**1446-1453.

Sjoberg A, Lutz M, Tannergren C, Wingolf C, Borde A, and Ungell AL (2013) Comprehensive study on regional human intestinal permeability and prediction of fraction absorbed of drugs using the Ussing chamber technique. *Eur J Pharm Sci* **48:**166-180.

Takenaka T, Harada N, Kuze J, Chiba M, Iwao T, and Matsunaga T (2014) Human small intestinal epithelial cells differentiated from adult intestinal stem cells as a novel system for predicting oral drug absorption in humans. *Drug Metab Dispos* **42:**1947-1954.

Yee S (1997) In vitro permeability across Caco-2 cells (colonic) can predict in vivo (small intestinal) absorption in man--fact or myth. *Pharm Res* **14:**763-766.

Zheng XE, Wang Z, Liao MZ, Lin YS, Shuhart MC, Schuetz EG, and Thummel KE (2012) Human PXR-mediated induction of intestinal CYP3A4 attenuates 1alpha,25-

dihydroxyvitamin D(3) function in human colon adenocarcinoma LS180 cells. *Biochem Pharmacol* **84:**391-401.

Footnotes

Funding:

This work was supported in part by the National Institutes of Health [Grants UH2 TR000504, TL1TR000422 (BDC) and R01 GM063666].

Current address:

1. Zhican Wang, Department of Pharmacokinetics and Drug Metabolism, Amgen Inc., South San Francisco, CA 94080, USA.

Figure Legends

Figure 1. Effect of rifampicin (RIF) and 1α,25-dihydroxyvitamin D3 (1α,25$(OH)_2D_3$) on the MDZ 1'-hydroxylation activities in LS180 (A), T84 (B), Caco-2 (C) and fSIEC (D). The cells were cultured on filter inserts for 9 days (fSIEC), 12 days (LS180 and T84 cells) or 19 days (Caco-2) then treated with vehicle (0.1% DMSO or 0.1% ethanol) or inducers (50 μM RIF or 1 nM 1α,25$(OH)_2D_3$) for 48 hours. Data represent the mean ± S.D. for three replicate cultures. *, $p < 0.05$, **, $p < 0.01$

Figure 2. Effects of rifampin (RIF) and 1α,25-dihydroxyvitamin D3 (1α,25$(OH)_2D_3$) on mRNA expression in LS180 (A), T84 (B) Caco-2 (C) and fSIEC (D) cells. The cells were cultured on permeable filter inserts for 9 days (fSIEC), 12 days (LS180 and T84 cells) or 19 days (Caco-2) then treated with vehicle (0.1% DMSO or 0.1% ethanol) or inducers (50 μM RIF or 1 nM 1α,25$(OH)_2D_3$) for 48 hours. Data are presented as a ratio of the GAPDH-normalized measurements obtained with inducer treatment compared to the vehicle (0.1% DMSO or 0.1% ethanol) treatment for 3 replicate cultures of both vehicle and inducer treatment groups. Error bars represent the standard deviation of the induction ratio as determined via a propagation of error calculation (Reckhow, 2004). * indicates statistical significance ($p < 0.05$) of the induction effect as determined unpaired t-test comparing treatment to its respective vehicle control.

Figure 3. Time-dependent transepithelial electrical resistance (TEER) development of LS180, T84, Caco-2 and small intestinal epithelial cells (fSIEC) grown on permeable filter support. Data represent mean ± S.D. for 3 replicate cultures.

Figure 4. Permeability coefficients (P_{app}) for the compounds transported by passive diffusion across filter-grown LS180, T84, Caco-2 and small intestinal epithelial cells (fSIEC). The cells were cultured on permeable filter inserts for 7 days (LS180 and T84), 9 days (fSIEC) or 21 days (Caco-2). Data is in arbitrary units and represent mean ± S.D. for three replicate cultures.

Figure 5. Cellular localization of tight junction protein ZO-1 in LS180 (A), T84(B), Caco-2 (C) and fSIEC (D) by confocal microscopy. The cells were cultured on permeable filter support for 7 days (LS180 and T84), 9 days (fSIEC) or 20 days (Caco-2). The cellular localization of ZO-1 was detected by a rabbit anti-ZO-1 antibody and an Alexa fluor 488 donkey anti-rabbit IgG secondary antibody (Green). Nuclei were counter-stained with DAPI (Blue).

Figure 1.

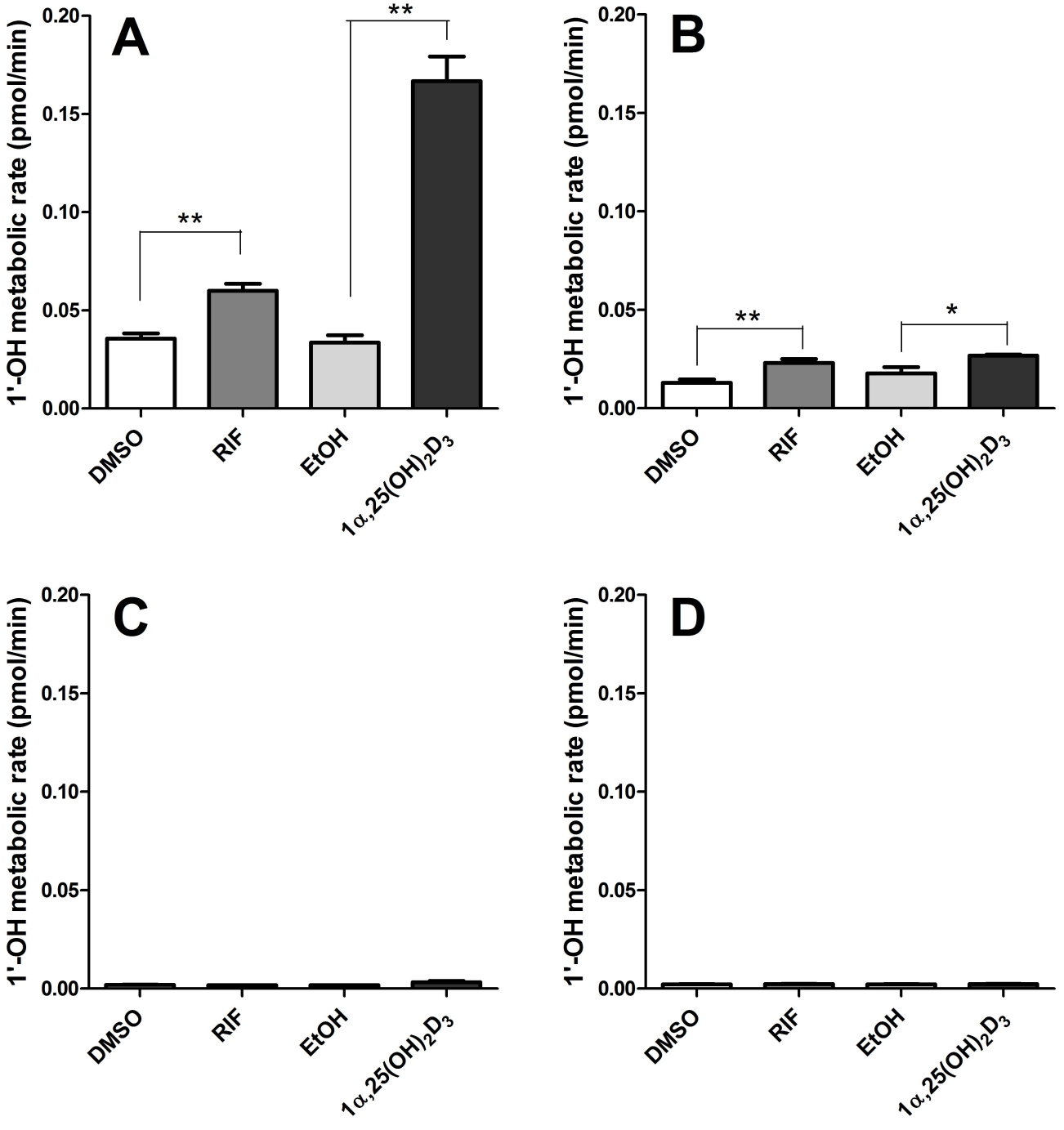
A
B
C
D
1'-OH metabolic rate (pmol/min)
0.20
0.15
0.10
0.05
0.00
**
*
DMSO
RIF
EtOH
1α,25(OH)2D3

Figure 2.

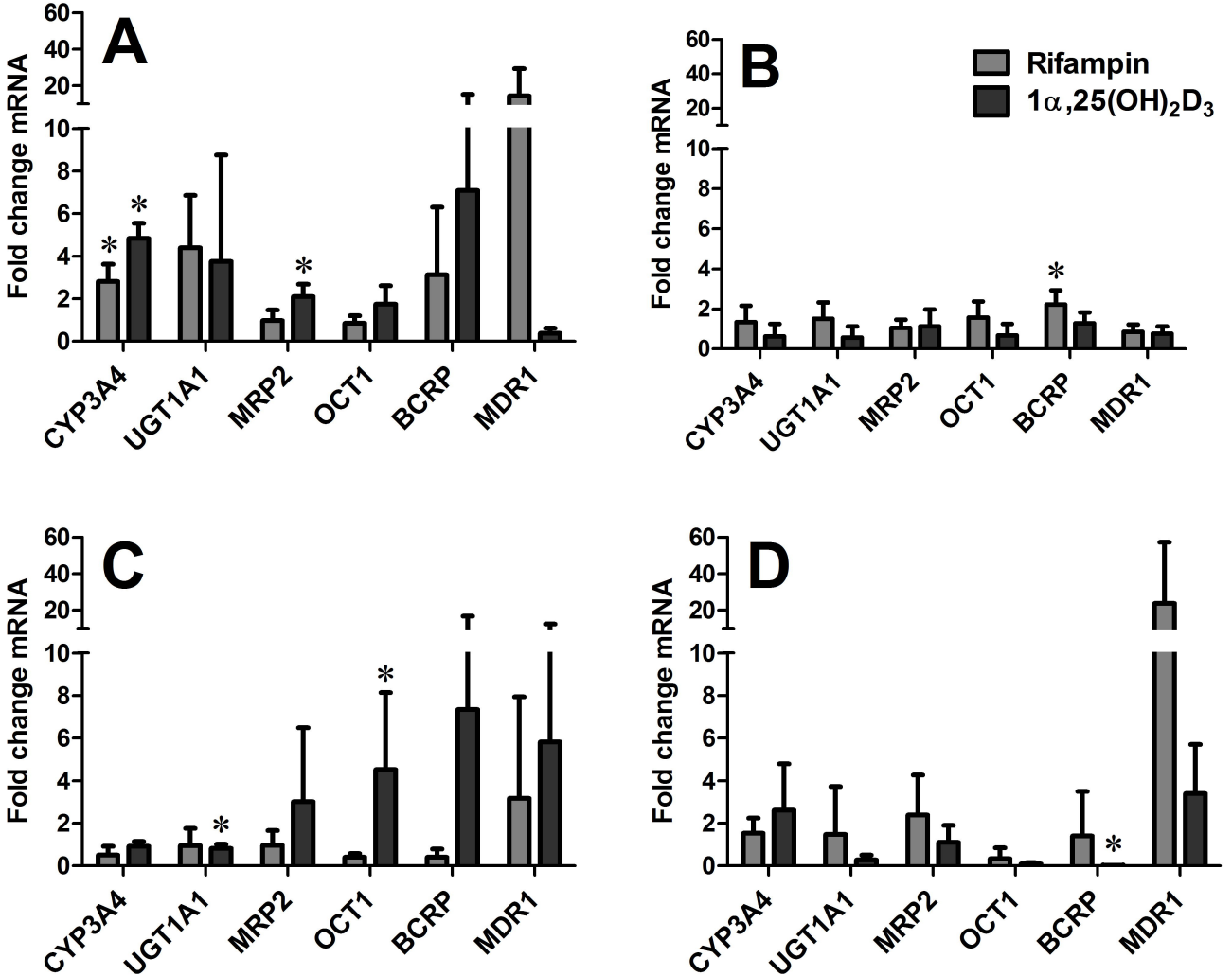
A
B
C
D
Fold change mRNA
Rifampin
1α,25(OH)2D3
CYP3A4
UGT1A1
MRP2
OCT1
BCRP
MDR1
0
2
4
6
8
10
20
40
60
*

Figure 3.

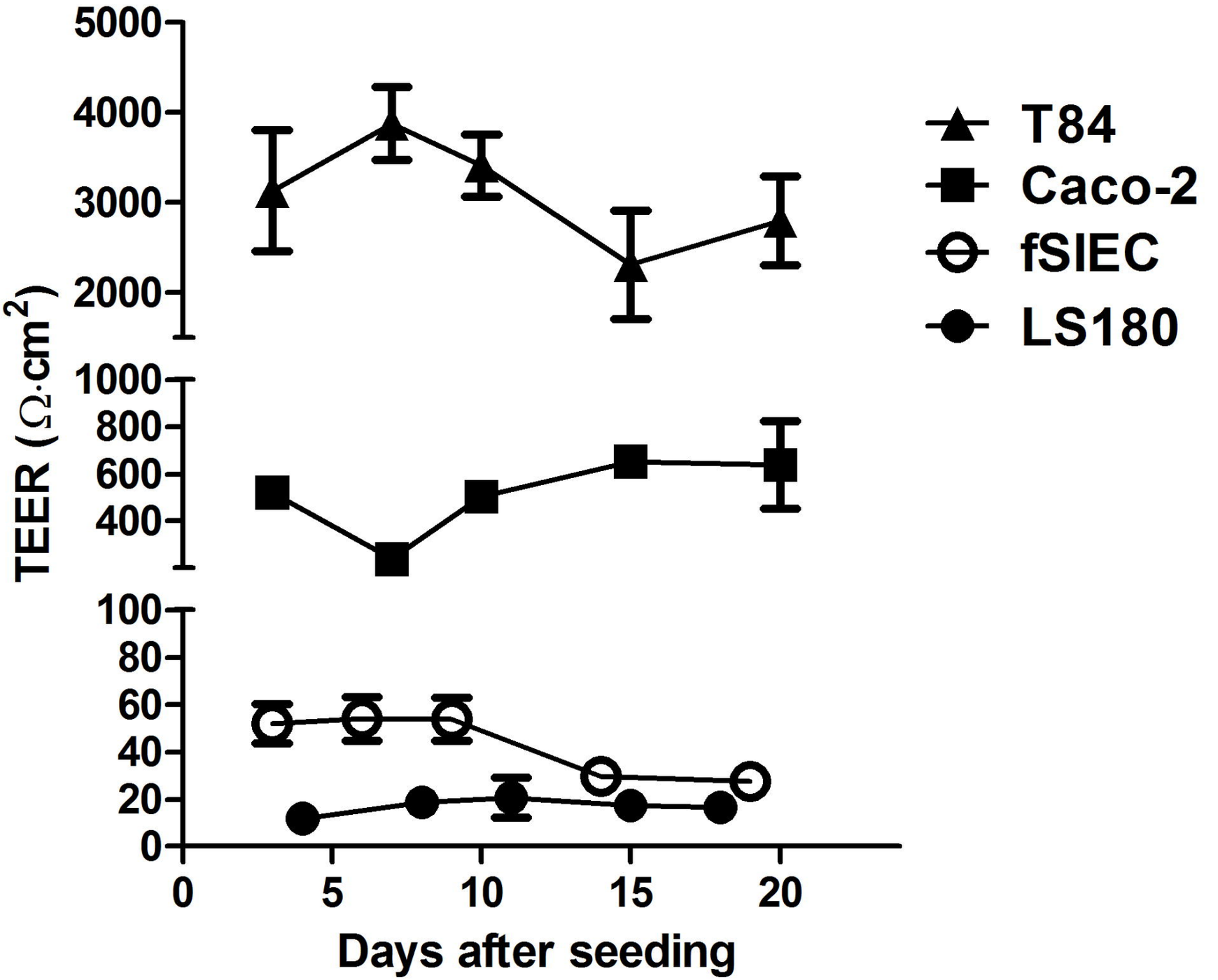
5000
4000
3000
2000
1000
800
600
400
100
80
60
40
20
0
TEER (Ω·cm²)
0
5
10
15
20
Days after seeding
T84
Caco-2
fSIEC
LS180

Figure 4.

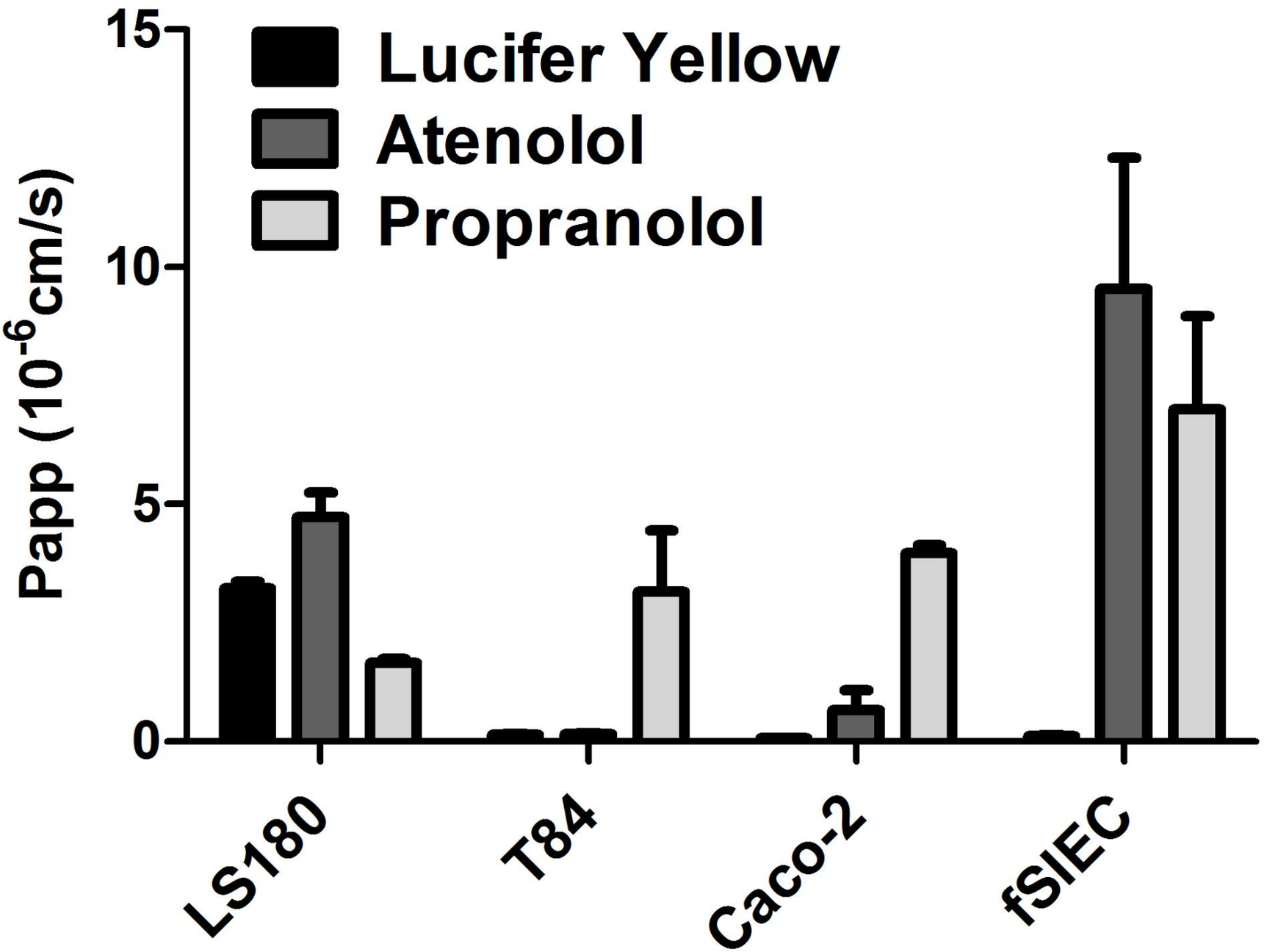
Lucifer Yellow
Atenolol
Propranolol
Papp (10^{-6}cm/s)
15
10
5
0
LS180
T84
Caco-2
fSIEC

Figure 5.